Diffusion and Partitioning of Proteins in Charged Agarose Gels

Erin M. Johnson,* David A. Berk,‡ Rakesh K. Jain,‡ and William M. Deen*

*Department of Chemical Engineering, Massachusetts Institute of Technology, Cambridge, Massachusetts 02139-4307, and ‡Department of Radiation Oncology, Massachusetts General Hospital and Harvard Medical School, Boston, Massachusetts 02114 USA

ABSTRACT The effects of electrostatic interactions on the diffusion and equilibrium partitioning of fluorescein-labeled proteins in charged gels were examined using fluorescence recovery after photobleaching and gel chromatography, respectively. Measurements were made with BSA, ovalbumin, and lactalbumin in SP-Sepharose (6% sulfated agarose), in phosphate buffers at pH 7 and ionic strengths ranging from 0.01 to 1.0 M. Diffusivities in individual gel beads (D) and in the adjacent bulk solution (D_∞) were determined from the spatial Fourier transform of the digitized two-dimensional fluorescence recovery images. Equilibrium partition coefficients (Φ) were measured by recirculating protein solutions through a gel chromatography column until equilibrium was reached, and using a mass balance. Diffusion in the gel beads was hindered noticeably, with $D/D_\infty = 0.4$–0.5 in each case. There were no effects of ionic strength on BSA diffusivities, but with the smaller proteins (ovalbumin and lactalbumin) D_∞ increased slightly and D decreased at the lowest ionic strength. In contrast to the modest changes in diffusivity, there were marked effects of ionic strength on the partition coefficients of these proteins. We conclude that for diffusion of globular proteins through gel membranes of like charge, electrostatic effects on the effective diffusivity ($D_{eff} = \Phi D$) are likely to result primarily from variations in Φ with only small contributions from the intramembrane diffusivity.

INTRODUCTION

Diffusive transport of macromolecules through gels is important in various chromatographic and membrane separation processes. For diffusion across any type of membrane, the driving force is usually expressed in terms of concentrations in the external solutions, so that the effective transmembrane diffusivity (D_{eff}) is given by

$$D_{eff} = \Phi D, \tag{1}$$

where Φ is the partition coefficient (the ratio of the intramembrane to the external concentration at equilibrium) and D is the diffusivity within the membrane phase. Accordingly, for a macromolecule in a gel membrane, D_{eff} tends to be lower than the free solution diffusivity (D_∞) for two reasons. First, hydrodynamic interactions between the macromolecular solute and the fibers that compose the gel medium reduce the mobility of the solute, making D lower than D_∞. Second, Φ is ordinarily less than unity due to steric and/or electrostatic interactions.

For uncharged gels, there is considerable experimental information on the partition coefficients of proteins and other macromolecules (Laurent, 1967; Crone, 1974; Dubin and Principi, 1989; Boyer and Hsu, 1992; Moussaoui et al., 1992;). Diffusivities within gels have received somewhat less attention, but available results clearly demonstrate that in neutral gels the macromolecular diffusivity is significantly reduced (Sellen, 1985; Jain et al., 1990; Moussaoui et al., 1992; Boyer and Hsu, 1992). With regard to theory, Ogston (1958) derived a relationship to predict Φ for uncharged, spherical macromolecules within a randomly oriented array of cylindrical fibers:

$$\Phi = \exp\left[-\phi\left(1 + \frac{r_s}{r_f}\right)^2\right], \tag{2}$$

where ϕ is the volume fraction of fibers, r_s is the radius of the sphere, and r_f is the radius of the fibers. This expression, which is limited to very dilute solutions, agrees well with reported values for Φ of proteins and Ficoll in neutral agarose gels (Laurent, 1967). More recently, Fanti and Glandt (1990) used a density-functional theory to verify independently the Ogston expression and to predict the partition coefficient for more concentrated solutions. To describe the reduced diffusivity of a spherical molecule within a random fiber matrix, Ogston et al. (1973) proposed a stochastic jump model, which leads to the expression

$$\frac{D}{D_\infty} = \exp\left[-\phi^{1/2}\frac{r_s}{r_f}\right]. \tag{3}$$

Equation 3, which has been used with some success to obtain semi-empirical correlations of diffusion data in gels (Ogston et al., 1973), does not consider hydrodynamic interactions between the mobile solute and the fibers. Phillips et al. (1989) suggested that hydrodynamic interactions are approximated using an effective medium approach, based on Brinkman's equation. The result was

$$\frac{D}{D_\infty} = \left[1 + \left(\frac{r_s^2}{\kappa}\right)^{1/2} + \frac{1}{3}\left(\frac{r_s^2}{\kappa}\right)\right]^{-1}, \tag{4}$$

where κ is the Darcy permeability of the fibrous medium.

Relatively little information is available on the partitioning or diffusion of charged macromolecules in charged gels. The effects of charge on D_{eff} for micelles (Johnson et al., 1989)

Received for publication 6 September 1994 and in final form 9 January 1995.

Address reprint requests to Dr. William M. Deen, Department of Chemical Engineering, 66-509, Massachusetts Institute of Technology, Cambridge, MA 02139. Tel.: 617-253-4535; Fax: 617-258-8224; E-mail: wmdeen@mit.edu.

0006-3495/95/04/1561/08 $2.00

and linear polyelectrolytes (Lin and Deen, 1992) in track-etch membranes with straight, cylindrical pores have been explained fully by theoretical predictions of the effects on Φ, suggesting that for macromolecules in such pores there is little or no effect of charge on D. The extent to which this might also be true for macromolecules in charged gels is unknown. Diffusion studies using charged probes in semi-dilute polymer solutions indicate that the effect of ionic strength on D is not negligible. In tracer diffusion studies of BSA in DNA solutions (Wattenbarger et al., 1992), it was found that, upon increasing the DNA concentration from 0 to 30 mg/ml, the diffusivity of BSA in a 0.01 M NaCl solution decreased more than in a 0.1 M NaCl solution. At 30 mg/ml DNA, the tracer diffusion coefficient of BSA in 0.01 M NaCl was about 20% lower than in 0.1 M NaCl. Studies of the diffusion of polystyrene latex spheres in polyacrylic acid solutions (Phillies et al., 1987, 1989) also showed that a decrease in ionic strength lowered the diffusion coefficient. Whether any of these results are applicable to gels of relatively fixed structure (e.g., charged agarose) is unclear.

The purpose of this study was to assess the relative importance of charge interactions for Φ and D, by measuring the effects of ionic strength on the partition and diffusion coefficients of selected proteins in a gel of like charge. We chose three commonly used globular proteins (BSA, ovalbumin, and lactalbumin) whose physical properties are fairly well characterized in the literature. Sulfated agarose gel was used, primarily because it is a rigid polysaccharide that does not swell or shrink when exposed to changes in ionic strength, so that the volume fraction of fibers remains constant. In addition, the acidity of the sulfate groups ensures that the amount of charge on the gel is essentially independent of pH.

MATERIALS AND METHODS

Proteins

Three fluorescein-labeled proteins, BSA (M_r 68,000), ovalbumin (M_r 45,000), and lactalbumin (M_r 14,200) were obtained from Molecular Probes (Eugene, OR). Aqueous samples were prepared by dissolving the fluorescent proteins (4 mg/ml) in 0.01 M sodium phosphate buffer, pH 7.1. The ionic strength was changed by adding either 0.10 or 1.00 M potassium chloride, yielding final ionic strengths (including the phosphate buffer) of 0.11 or 1.01 M. Size exclusion chromatography of each sample showed that there was no detectable free fluorescein present. The net charge of each protein was calculated by using published titration curves for the unlabeled protein, and by adjusting for the contribution of the carboxyl group on the fluorescein. The average number of fluorescein groups per protein molecule was reported by Molecular Probes to be 5.3, 2.3, and 1.3 for BSA, ovalbumin, and lactalbumin, respectively, and the pK_a of the fluorescein carboxyl was taken to be 6.5 (Haugland, 1992). The size and charge characteristics of the proteins are summarized in Table 1. The Stokes-Einstein radii in Table 1 are based on free solution diffusivities from the literature, as discussed in more detail later.

Gel beads

SP-Sepharose Big Beads, a 6% sulfated agarose gel, was obtained from Pharmacia (Piscataway, NJ). The diameters of the hydrated gel beads ranged between 100 and 300 μm. The charge on the SP-Sepharose was 0.23 meq/ml packed bed, as determined by titration by Pharmacia. Using the void and total volumes of the packed bed, the volume fraction of fibers, and an agarose fiber radius of 1.9 nm (see Appendix), the surface charge density was 0.42 C/m^2. The gel beads were washed and suspended in 0.01 M sodium phosphate buffer, pH 7.1.

TABLE 1 Protein characteristics

Protein	Stokes radius (nm)	Isoelectric point (pI)	Native protein charge	Fluorescein charge	Net protein charge
BSA-fluorescein (Lot # 6531–1)	3.5	4.9*	−33[§]	−4.1	−37
Ovalbumin-fluorescein (Lot # 6521–1)	2.8	4.7*	−17[¶]	−1.8	−19
Lactalbumin-fluorescein (Lot # 6511–1)	2.0	5.1[‡]	−8‡	−1.0	−9

*Righetti and Caravaggio (1976).
[‡]Shukla (1973).
[§]Tanford et al. (1955).
[¶]Overbeek (1950).

Diffusion measurements

Samples for diffusion measurements were prepared by combining the gel bead suspension, the fluorescent protein, and potassium chloride to a final protein concentration of 1 mg/ml, and allowing the suspension to equilibrate. The suspension was then drawn into rectangular glass microslide chambers with dimensions of 0.3 × 3 × 50 mm (Vitro Dynamics, Rockaway, NJ), using a syringe attached to the microslide by silicon tubing. The ends of the microslide were blocked with a sealing compound (Hemato-seal, Fisher, Pittsburgh, PA).

Diffusion coefficients were determined by an image-based fluorescence recovery after photobleaching (FRAP) technique. We have established previously the reliability of the method for measurements of diffusion in agarose gels, independent of light scattering effects, in samples of 50–400 μm thickness (Berk et al., 1993). The primary reason that the image-based FRAP technique using a spatial Fourier transform analysis is more accurate in gels is that this technique is insensitive to the actual bleached radius. In gels that scatter light, the bleached radius changes as a function of gel thickness. The consequent uncertainties in the true bleached radius make it difficult to obtain reliable results using a direct photometric analysis. The sample was placed on the stage of an upright microscope (Universal, Zeiss, Thornwood, NY) equipped for epi-fluorescence. The excitation filter (485 ± 11 nm, band-pass), dichroic mirror (505 nm), and barrier filter (530 nm, long-pass) are designed for fluorescein observation. By means of a beam splitting mirror, epi-illumination was provided by both a conventional mercury arc lamp (100 W lamp, Osram, Munich; with stable power supply and convection-cooled housing, models 68806 and 60000, Oriel Corp., Stratford, CT) and by an argon laser (model 2020, Spectra Physics, Mountain View, CA). The laser operated in the TEM00 mode (i.e., the intensity obeyed a radially symmetric Gaussian profile). The beam was directed through the microscope epi-illumination port to the back focal plane of the objective. With the 20×, NA 0.4 objective used for these experiments, the laser spot radius in a thin layer of aqueous solution (the Gaussian radius of the attenuated beam projected onto a 50-μm-thick layer of FITC solution) was 20 μm. The microscope image was projected directly to an intensified CCD camera (model 2400, Hamamatsu, Japan). Fluorescence images were digitized directly (DT-2851 image processing board: Data Translation, Marlboro, MA; in an IBM PC-AT computer, Boca Raton, FL) and stored at a rate of 5 images/s. Only the central portion (100 × 125 pixels) of the full 512 × 480 pixel image was stored for analysis. An electronic shutter in the laser light path and another directly before the camera allowed automated computer control of the laser exposure time and image collection sequence. The spatial sampling rates (vertical and horizontal distances between pixels: 0.917 and 1.13 μm, respectively) were calculated from an image of a stage micrometer. Sources of error in the pixel dimensions were the uncertainty

in aligning a cursor on a micrometer line (each line is several pixels wide), and the possibility that the micrometer was not aligned exactly horizontally or vertically. The error was probably <5%.

For each protein at each ionic strength, diffusion measurements were made with five separate gel beads. For any given agarose bead, seven measurements each were made of D and D_∞. For the gel diffusivity (D) measurements, the bead was positioned so that its center was in the focal plane and directly in the laser path. To measure D_∞, the slide was moved laterally so that no beads appeared in the image. After a brief exposure to laser illumination (30 ms), the sample was observed under conventional epifluorescence illumination and the digitized fluorescence images were stored for later analysis. The fluorescence intensity in a region of the image far ($\geq$200 μm) from the laser spot was also monitored, to detect the occurrence of photobleaching by the conventional light source; this additional bleaching was in the range of 0–2% of the total intensity over a 30-s monitoring period. To allow for complete recovery of the bleached areas, the gel diffusion measurements were alternated with the free solution diffusivity measurements. The room temperature was recorded (23–29°C), and all diffusion coefficients were corrected to 20°C using the Stokes-Einstein relation and an interpolation of the viscosity of water given by the CRC handbook (Weast and Astle, 1980).

Analysis of FRAP data

The diffusion coefficient was determined by a spatial frequency analysis of successive images (Berk et al., 1993; Tsay and Jacobson, 1991). Each post-bleach image was first subtracted from the initial pre-bleach image, then subjected to a two-dimensional discrete Fourier transform. To reduce the high frequency components due to truncation of the image (Gibbs phenomenon), we used an image padding and windowing algorithm. First, the original 100 × 125 pixel image array, $i(j,k)$, was expanded to a 200 × 250 array by adding a border (see Appendix). Then this array was multiplied by a windowing function to give

$$i_w(j,k) = \frac{i(j,k)}{4}\left[1 - \cos\left(2\pi\frac{j-1}{m-1}\right)\right]\left[1 - \cos\left(2\pi\frac{k-1}{n-1}\right)\right], \quad (5)$$

where m and n are the dimensions of the extended array. The processed image array was then subjected to a discrete Fourier transform (two-dimensional fast Fourier transform subroutine; IMSL, Houston, TX) to obtain an array of complex Fourier coefficients, which were converted into magnitudes, $I(j,k)$. Discrete spatial frequencies, u and v, were then calculated from the indices j and k. The diffusion coefficient, D, was calculated from the decay of each Fourier coefficient in successive images:

$$\frac{I(u,v,t)}{I_0} = \beta + (1-\beta)\exp(-4\pi^2q^2Dt), \quad (6)$$

where q is the magnitude of the frequency ($q^2 = u^2 + v^2$), β is a parameter that accounts for incomplete recovery of the fluorescence (see below), and $I_0 \equiv I(u, v, 0)$. The decay of the coefficients corresponding to the lowest four frequencies was meaningless because of the padding and windowing process, but the next 20–30 components were observed to decay at approximately the same frequency-scaled rate. An initial estimate of D was obtained by the simultaneous fitting of several Fourier coefficients to Eq. 6 by a nonlinear least-squares method. For a fit of N Fourier components to the diffusional decay, there are $N + 2$ independent parameters: the diffusion coefficient, D, the recovery parameter, β, and N separate initial values, I_0. To maximize signal-to-noise ratio and temporal resolution, we chose the five lowest usable frequency components, because they had the greatest magnitude and decayed at the slowest rate. The estimate of D was refined by re-plotting these components in the form

$$f(t) \equiv -\ln\left[\frac{(I/I_0) - \beta}{1-\beta}\right] = 4\pi^2q^2Dt \quad (7)$$

and performing a linear fit with I_0 and β fixed. Linear regression of $f(t)$ vs. t was restricted to early times, such that $f(t) \leq 1$.

Fig. 1 *a* illustrates typical results from an analysis of a single photobleaching recovery for diffusion in free solution and within a gel bead. The diffusion coefficients in free solution and in the gel phase calculated from the decay of individual Fourier components are shown in Fig. 1 *b*. The absence of a strong dependence of D on spatial frequency indicates that the method indeed measured diffusion within the bead and not within the free solution. If the fluorescence recovery was influenced by diffusion outside the bead volume, the lower frequency components, which contain more of the out-of-focus signal, would decay at a faster scaled rate and give higher diffusivity values. For each fit of an individual component, the SE of the diffusion coefficient was typically 5–10%, although some components could not be fit (SE > 50%). When five or more components were combined for a global fit, as shown in Fig. 1 *a*, the SE of the estimate was only 1–2% and the correlation coefficient r^2 was at least 97%.

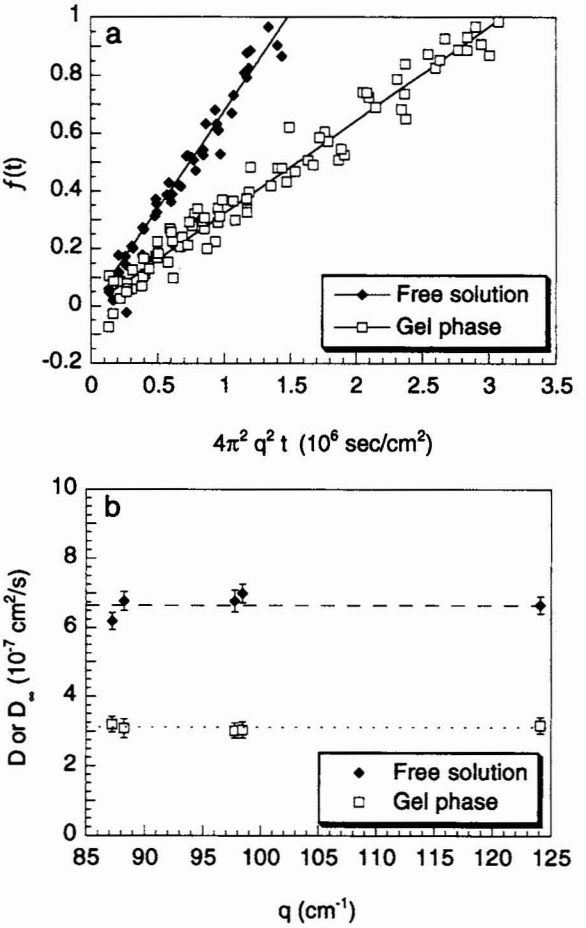

FIGURE 1 Calculation of diffusion coefficient in a gel bead from one photobleaching recovery sequence, for BSA at an ionic strength of 1 M. The temperature was 28.7°C. (*a*) The diffusion coefficient was calculated for each Fourier component for the free solution (◆) and for the gel phase (□), and overall diffusion coefficients were calculated by a global fit to Eq. 7 incorporating several components (——). (*b*) The individual diffusivity values at higher spatial frequencies are not significantly lower than the overall value. This is evidence that the overall value is a valid measure of diffusion within the bead and that the method is not sensitive to photobleaching in the surrounding free solution.

The parameter β introduced in Eq. 6 is equivalent in principle to the fraction of the total protein that is immobile. Its values typically were between −3 and +8% for the free solution measurements and between 8 and 15% for the diffusion measurements in the gel beads. The results obtained for free solution, where no adsorption could be present, indicate that small non-zero values are without physical significance, and evidently arise from signal processing difficulties. Because the signal-to-noise ratio was lower

in the gel media (the gel tended to scatter some of the light), the somewhat larger values of β probably do not reflect actual adsorption of protein on the gel beads. To distinguish between a true immobile fraction and noise-related artifacts, we compared the results obtained by using either the pre-bleach image or the final post-bleach image (after the diffusional recovery was essentially complete) as a reference. The amount of photobleaching was quantified by subtracting each spot image from the reference image (either the pre-bleach or the final image). When the pre-bleach image is used as the reference, the resulting differential image shows the total amount of photobleaching, including any immobile component. The final post-bleach image retains a residual spot due to the immobile component (if any), so that the differential image relative to this reference should measure only the amount of photobleaching that affected mobile molecules. In other words, the differential image obtained with this second reference should decay entirely, independent of any immobile fraction. We found that both reference images yielded virtually identical diffusion coefficients and β values. We conclude that the true immobile fraction was less than 1%.

There was bleaching not just within the gel beads but also in the free solution above and below them, making it necessary that the free solution be sufficiently out of focus so as not to contaminate the image and influence the analysis. Berk et al. (1993) showed that if the free solution is at least 100 μm from the focal plane, its effects on the diffusivity measurements are negligible. The analysis area used here was a 115 $\times$ 115 μm^2 centered on the bead and focused at the midplane. To ensure that the free solution was at least 100 μm from the recorded area, only agarose beads with diameters greater than 240 μm were examined.

Partitioning measurements

Equilibrium partition coefficients were measured using a C-10/20 chromatography column (Pharmacia) containing approximately 12 ml of SP-Sepharose Big Beads. The column had a sample applicator at the inlet and was connected to a peristaltic pump; the applicator and tubing volumes were 3.0 and 0.1 ml, respectively. A sample of volume V_i = 3.0 ml with an initial concentration C_i of ~0.25 mg/ml of fluorescent protein was loaded on the column, and the eluent was recirculated at 0.5 ml/min. After the whole system had equilibrated (2 h), the final protein concentration C_f was measured in a 1-ml sample withdrawn from the sample applicator. Protein concentrations were determined by measuring the absorbance of the sample using a Shimadzu (Columbia, MD) UV-Vis spectrophotometer at 488 nm. A calibration curve for determining the final concentration was made by making dilutions of the initial sample. Preliminary experiments performed by recirculating the eluent through a flow cell in the UV spectrophotometer confirmed that equilibration was reached within 90 min. The void volume (V_0, the total liquid volume outside the gel beads, including the flow loop) was determined similarly by recirculating fractionated blue dextran (M_r 2 $\times$ 10^6). The equilibrium partition coefficient was calculated using an overall mass balance, as

$$\Phi = \frac{C_i V_i - C_f V_0}{(V_t - V_0)C_f}, \quad (8)$$

where V_t = 15.1 ml is the total volume (V_0 plus bead volume).

Statistical calculations

For both the diffusion and partition coefficients, statistical differences as a function of ionic strength were assessed using ANOVA. In addition, the protein diffusivities for the three ionic strengths were compared using Tukey's method of multiple comparisons (Larson and Marx, 1986). Differences at the 95% confidence level were judged to be significant. Uncertainties in the diffusion and partition coefficients are reported as SDs.

RESULTS

Diffusivities

The free solution and gel diffusivities for each protein at the three ionic strengths are summarized in Table 2. There was no effect of ionic strength on D_∞ for albumin, whereas for ovalbumin and lactalbumin D_∞ exhibited slight (but statistically significant) increases at the lower ionic strengths. The maximum variation in D_∞ with ionic strength was 7%, for lactalbumin. The free solution diffusivities are compared with literature values in Table 3. Because the effects of ionic strength on D_∞ were minimal, the FRAP values in Table 3 were calculated by pooling all of the present data. The values of D_∞ obtained here with fluorescein-labeled proteins are seen to be about 10% lower than typical values measured for unlabeled proteins using a variety of methods. A systematic error of this magnitude might be caused by the propagation of error in the spatial frequencies caused by an error in the measurement of the pixel distance. A 5% error in pixel dimensions (the maximum error that is likely to have occurred) would yield a 10% error in diffusivities. This would not affect the diffusivity ratio, D/D_∞ because we used the same frequencies for both the free solution and gel phase diffusion measurements. It is also possible that the addition of the fluorescein groups caused a noticeable increase in the hydrodynamic radii of the proteins, thereby lowering the true values of D_∞. In other words, the error in the FRAP values for D_∞ may not be as large as 10%. In calculating the Stokes-Einstein radii shown in Table 1, we chose to use the averages of the literature values of D_∞. (The value for BSA reported by Giddings et al. (1976), which is 13% below the average of the other literature values, was excluded.)

Returning to the results in Table 2, for all three proteins the gel diffusion coefficients were substantially lower than the corresponding free solution diffusivities. As with D_∞, the value of D for albumin was not affected by ionic strength.

TABLE 2 Partitioning and diffusivity of proteins in SP-Sepharose

Protein	Ionic strength (M)	D_∞ (10^{-7} cm^2/s)	D (10^{-7} cm^2/s)	D/D_∞	Φ
BSA	1.01	5.7 ± 0.2^a	2.7 ± 0.4^b	0.47 ± 0.07^c	0.67 ± 0.03
	0.11	5.8 ± 0.4^a	2.6 ± 0.2^b	0.45 ± 0.05^c	0.47 ± 0.01
	0.01	5.7 ± 0.2^a	2.6 ± 0.4^b	0.45 ± 0.07^c	0.29 ± 0.01
Ovalbumin	1.01	6.7 ± 0.3	3.1 ± 0.2^e	0.47 ± 0.05^f	0.64 ± 0.02
	0.11	6.8 ± 0.2^d	3.0 ± 0.2^e	0.44 ± 0.04^f	0.59 ± 0.01
	0.01	6.8 ± 0.4^d	2.8 ± 0.5	0.41 ± 0.06	0.29 ± 0.02
Lactalbumin	1.01	9.2 ± 0.5^g	4.9 ± 0.2	0.53 ± 0.09	0.78 ± 0.03
	0.11	9.3 ± 0.8^g	4.5 ± 0.2	0.49 ± 0.05	0.75 ± 0.04
	0.01	9.9 ± 0.6	3.8 ± 0.4	0.38 ± 0.04	0.44 ± 0.03

Diffusivities have been corrected to 20°C using the Stokes-Einstein equation. Values are given as mean ± SD Common superscripts indicate that quantities are not statistically different (95% confidence level).

TABLE 3 Comparison of free solution diffusivities to literature values (20°C)

Protein	D_∞ (10^{-7} cm^2/s) FRAP	Literature	Literature method*	Reference
BSA	5.7 ± 0.2	5.3	Flow fractionation	Giddings et al. (1976)
		5.8 ± 0.1	Rayleigh light scattering	Sellen (1973)
		5.9	Hydrodynamic stability	Anderson et al. (1978)
		6.0 ± 0.1	QELS	Bor Fuh et al. (1993)
		6.1 ± 0.1	QELS	Raj and Flygare (1974)
		6.2 ± 0.4	Flow fractionation	Bor Fuh et al. (1993)
		6.3 ± 0.1	QELS	Gaigalas et al. (1992)
		6.3 ± 0.1	Taylor dispersion	Walters et al. (1984)
		6.4 ± 0.9	FRAP	Jain et al. (1990)
Ovalbumin	6.7 ± 0.3	7.2 ± 0.2	Taylor dispersion	Walters et al. (1984)
		7.4	PFG NMR	Gibbs et al. (1991)
		7.7 ± 0.4	Flow fractionation	Bor Fuh et al. (1993)
		7.9 ± 0.2	QELS	Bor Fuh et al. (1993)
Lactalbumin	9.2 ± 0.5	10.6	Sedimentation-diffusion	Gordon and Semmett (1953)

*QELS = quasi-elastic light scattering; PFG = pulsed field gradient.

The values of D for ovalbumin and lactalbumin decreased by moderate amounts at low ionic strengths, with maximum changes of 10 and 23%, respectively. The diffusivity ratio, D/D_∞, for all three proteins ranged from about 0.4 to 0.5 and exhibited the same trends with ionic strength as did D.

Partition coefficients

The partition coefficients for the proteins at the three ionic strengths are summarized in Table 2. For all three proteins, there was a marked decrease in Φ with decreasing ionic strength. This is the expected trend for proteins and gels of like charge, because there will be less screening of the repulsive electrostatic interactions at the lower ionic strengths.

DISCUSSION

The objective of this study was to compare the effects of electrostatic interactions on the diffusion and equilibrium partitioning of charged macromolecules in gels of like charge. The experimental design allowed both diffusivities and partition coefficients to be measured independently using identical gel beads. We are unaware of any previous data on charge effects in gels where both quantities were measured using the same test macromolecules and gels, under the same conditions. A particular advantage of the FRAP method is that direct comparisons could be made of diffusivities measured in gel beads and in the adjacent bulk solution. For the three anionic proteins (bovine serum albumin, ovalbumin, and lactalbumin) in sulfated agarose gels, there was a much stronger effect of ionic strength on the partition coefficient (Φ) than on the gel diffusivity (D), indicating that electrostatic interactions have a greater effect on partitioning. This suggests that the effects of charge on the effective diffusivity of a globular protein through a gel membrane (ΦD) will result primarily from alterations in Φ.

A consideration of length scales suggests that charge effects on Φ should be important at the lower ionic strengths studied, but probably not at the highest ionic strength. Using the distribution of spacings calculated by Ogston (1958) for a random array of fibers, we estimate that the average distance between agarose fibers in the 6% gels studied was 11 nm (see Appendix). The Debye length, the characteristic length for electrostatic interactions in electrolyte solutions, ranged from 3 nm at 0.01 M ionic strength to 0.3 nm at 1 M. Thus, at the lowest ionic strength the Debye length was a significant fraction of the interfiber spacing, and a protein molecule located at almost any sterically allowed position in the gel should have experienced some electrostatic repulsion. In contrast, the small ratio of Debye length to interfiber spacing at 1 M should have resulted in minimal electrostatic interactions. A comparison of the measured values of Φ with those predicted by Ogston's partitioning theory for neutral spheres in random arrays of uncharged fibers suggests that this was the case. As shown in Fig. 2, the values of Φ measured in the 1 M buffer agree well with those predicted by Eq. 2. The values of r_f and ϕ needed for this calculation were estimated as described in the Appendix. As already mentioned, the Ogston theory generally agrees well with previous measurements of Φ for uncharged macromolecules in neutral agarose gels (Laurent, 1967).

For all three proteins, the gel diffusion coefficient, D, was significantly reduced when compared with the free solution diffusivity, D_∞. At the highest ionic strength, the values of D/D_∞ varied little among the proteins, ranging only from 0.47 to 0.53. However, the effects of ionic strength on D or D/D_∞ varied considerably, the magnitude of the changes following the order lactalbumin > ovalbumin > albumin. Thus, the effects of ionic strength on the gel diffusivity seemed to depend inversely on the Stokes-Einstein radius of the protein. This trend may be coincidental, in that other molecular properties (e.g., shape and charge density) may also influence protein mobility within the gel phase. If it is assumed that charge effects were minimal at the highest ionic strength, then it is legitimate to compare the measured values of D/D_∞ with those predicted by Eqs. 3 and 4. The value of κ needed in Eq.

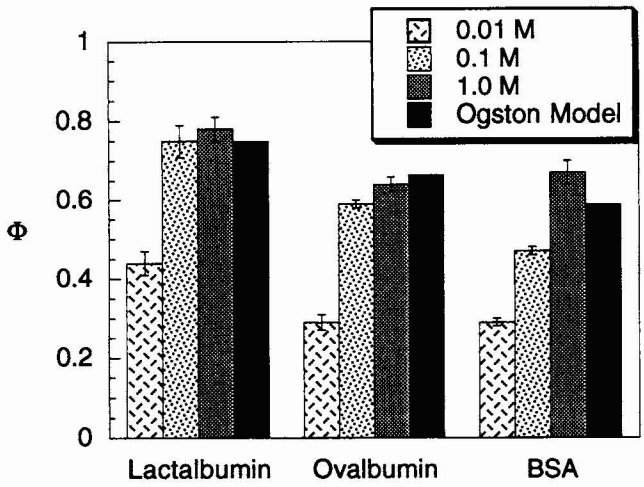

FIGURE 2 Comparison of measured values of the partition coefficient with those predicted using the theory of Ogston (1958), Eq. 2. The partition coefficients are shown as mean ± SD. The theory (developed for uncharged macromolecules and fibers) agrees well with the data at the highest ionic strength (1 M), where the electrostatic interactions are almost completely screened.

4 was estimated using a correlation given by Jackson and James (1986) for the hydraulic permeability of three-dimensional arrays of fibers:

$$\frac{\kappa}{r_f^2} = -\frac{3}{20\phi}(\ln \phi + 0.931). \quad (9)$$

With $r_f = 1.9$ nm and $\phi = 0.059$ (see Appendix), Eq. 9 gives $\kappa = 17.4\ \text{nm}^2$. As shown in Fig. 3, Eq. 3 (the Ogston diffusion model) consistently overestimated the value of D/D_∞ at 1 M and also predicted a larger effect of molecular radius than was observed. Eq. 4 (the Brinkman model) gave more accurate values of D/D_∞ for these conditions, but it too predicted a greater sensitivity to molecular radius. It should be noted that the better predictions obtained with the effective medium theory (Brinkman model) may be fortuitous, in that the values of κ were estimated from Eq. 9, rather than being measured for our specific gels.

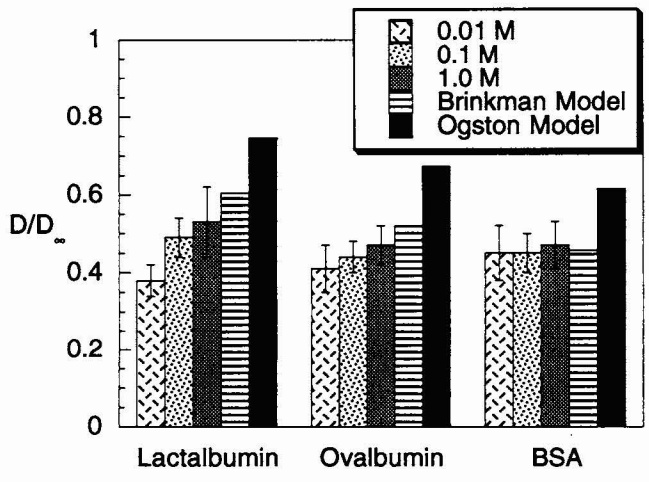

FIGURE 3 Comparison of measured values of reduced diffusivity (D/D_∞) with those predicted using Eq. 3 (Ogston diffusion model) and Eq. 4 (Brinkman model). The reduced diffusivities are shown as mean ± SD. The agreement between theory and data at 1 M is better with the Brinkman model, but both theories show greater sensitivity to molecular size than do the experimental results.

Equations 2–4 were intended to apply only to uncharged systems, and it is clear that additional theoretical work is needed to describe electrostatic effects on partitioning and diffusion in charged gels or other charged, fibrous media. Our finding that ionic strength tended to have a much more pronounced effect on Φ than on D/D_∞ suggests that it would be especially useful to devote attention to the effects of charge on equilibrium partitioning. The good agreement between the Ogston partitioning theory and data obtained when charge effects are absent suggests that the geometric model used, consisting of randomly oriented, cylindrical fibers, provides a good point of departure in modeling the effects of charge on Φ. Of course, more predictive theories for D/D_∞ of macromolecules in gels, both in neutral and in charged systems, are also needed.

The authors are grateful for the technical assistance provided by Jennifer Majernik.

This work was supported by grants from National Institutes of Health (DK20368 and R35-CA-J6591).

APPENDIX

Padding and windowing of the discrete fluorescence image

In this image-based fluorescence recovery technique, the diffusion coefficient is calculated from the decay of Fourier coefficients in successive images. This approach is advantageous for two reasons: first, it reduces sensitivity to out-of-focus light because the resultant image distortion affects only the relative magnitude of each Fourier coefficient but not the rate of its decay; and second, solution of the diffusion equation is simplified in Fourier space. However, one potential source of artifact is the use of a discrete Fourier transform to approximate the true transform. In particular, the truncation of the finite image gives rise to spurious high frequency components (leakage or Gibb's phenomenon) that are unrelated to the actual image and therefore interfere with the diffusion fit. We used two strategies to overcome this problem: padding and windowing.

A discrete Fourier transform actually represents an infinitely repeating two-dimensional array of the image. Fig. 4 *a* shows a one-dimensional illustration of this feature: a discontinuity may exist at the boundary between image elements. Ideally, the intensity of a processed image should smoothly approach zero at the periphery, because it is a differential image (pre-bleach minus post-bleach), but in practice there are spatial and temporal fluctuations in lamp intensity, detector gain, and out-of-focus fluorescence signal. To reduce this edge discontinuity effect, the image was multiplied by a two-dimensional hanning function (Brigham, 1974). This windowing function smoothly attenuates the image borders to zero.

It is important for the validity of the windowing approach that the size of the photobleached spot be less than the size of the image. In these experiments, the spot diameter in the gel bead was approximately 50 μm, compared with an image size of 115 × 115 μm. To minimize further the distortion of the spot intensity profile, the image was padded before the windowing step to produce a larger effective image size. At each edge of the image, a new border was added; this border was a symmetric reflection of the original image, as illustrated in Fig. 4 *b*. The resulting padded image was twice the size of the original image, but the infinite waveform described

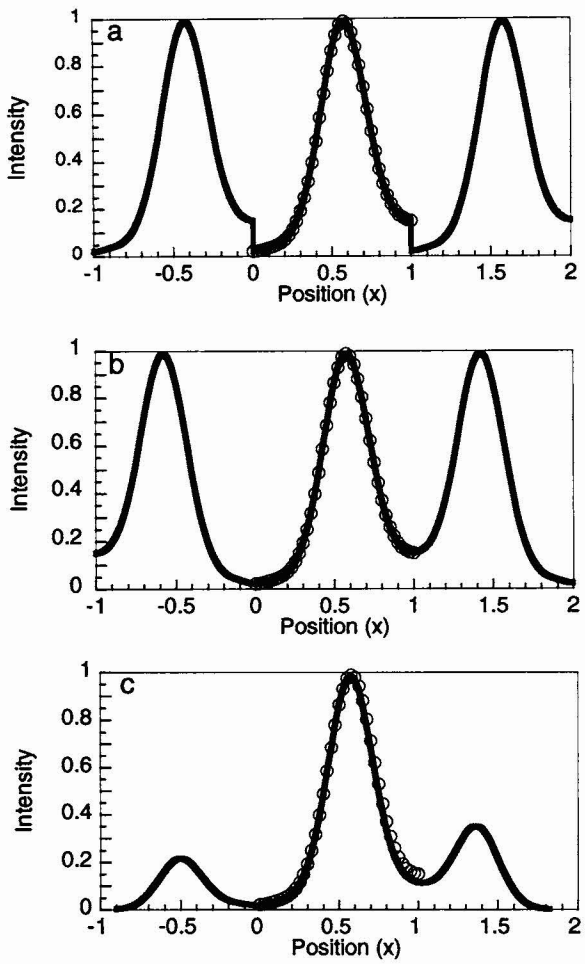

FIGURE 4 Illustration in one dimension of the padding and windowing algorithm for calculation of discrete Fourier transform (DFT) coefficients. The circles represent digitized image data corresponding to a photobleached spot (the original unbleached image minus the post-bleach image). Position (x) is scaled by the length of the data window. (a) The DFT of the data over the range $x = 0$–1 represents the infinite waveform shown by the line. The discontinuities at $x = 0$ and $x = 1$ cause spurious Fourier coefficients at high frequencies. (b) The data are reflected about the axes $x = 0$ and $x = 1$, doubling the period to $x = -0.5$ to 1.5. The infinite waveform corresponding to the new DFT is now continuous. (c) A windowing function smoothly attenuates the borders with minimal distortion to the spot intensity profile.

by the discrete Fourier transform of the image is similar to one produced without padding, except that the padded waveform had no discontinuities. The discrete Fourier transform of the padded image is no less accurate a representation of the true image; the advantage of this procedure is that the padded image can be windowed with less distortion of the spot at the center of the image.

Physical parameters for agarose gels

Agarose physically cross-links into branched bundles of fibers consisting of α-helical chains (Arnott et al., 1974), so that the agarose fiber radius used in the analysis is necessarily an average. To characterize the fiber radii, researchers have used several techniques, including light scattering (Obrink, 1968), SAXS (Djabourov, 1989), and electron microscopy (Spencer, 1982; Amsterdam et al., 1975; Waki et al., 1982; Whytock and Finch, 1991). The electron microscopy techniques give a range of fiber radii of 1–20 nm, but do not quantify the distribution of fiber sizes. Results from light scattering indicate that the average fiber radius is between 1.5 and 2.0 nm, whereas the SAXS results give a bimodal distribution of 87% fibers with 1.5-nm radius and 13% with 4.5-nm radius, yielding an average radius of 1.9 nm. The SAXS result is consistent with the values given using light scattering. Accordingly, for use in Eqs. 2–4 we chose $r_f = 1.9$ nm.

The agarose fibril is a helix with internally bound water (Arnott et al., 1974), so that the volume fraction of fibers cannot be obtained directly from the agarose concentration and the dry density. For this structure, Arnott and co-workers determined that the hydrated chain density is 1.4 g/ml. With a dry agarose density, ρ_a, of 1.64 g/ml (Laurent, 1967) and a water density of 1.0 g/ml, the mass fraction of agarose in the fiber, ω_a, is 0.625. Denoting the mass concentration of agarose as C_a, the volume fraction of fibers in the gel can be determined by

$$\phi = \frac{C_s}{\rho_a \omega_a}. \tag{10}$$

Using Eq. 10, the volume fraction of fibers in a 6% (by weight) agarose gel is $\phi = 0.059$. Thus, coincidentally, the volume fraction of fibers is almost identical to the weight fraction of agarose.

Ogston (1958) derived a probability density function for the distance H from an arbitrary point to the surface of the nearest fiber in a random array. The result may be expressed as

$$g(H) = \frac{2\phi(H + r_f)}{r_f^2} \exp\left(\frac{-\phi(H + r_f)^2}{r_f^2}\right). \tag{11}$$

We computed the average distance to the closest fiber, $\bar{H}$, using

$$\bar{H} = \frac{\int_0^\infty H\, g(H)\, dH}{\int_0^\infty g(H)\, dH}. \tag{12}$$

With $\phi = 0.059$ and $r_f = 1.9$ nm, the average distance to the closest fiber is 5.4 nm. The average fiber spacing was estimated as $\bar{H}$, or 11 nm.

REFERENCES

Amsterdam, A., Z. Er-El, and S. Shaltiel. 1975. Ultrastructure of beaded agarose. *Arch. Biochem. Biophys.* 171:673–677.

Anderson, J. L., F. Rauh, and A. Morales. 1978. Particle diffusion as a function of concentration and ionic strength. *J. Phys. Chem.* 82:608–616.

Arnott, S., A. Fulmer, W. E. Scott, I. C. M. Dea, R. Moorhouse, and D. A. Rees. 1974. The agarose double helix and its function in agarose gel structure. *J. Mol. Biol.* 90:269–284.

Berk, D. A., F. Yuan, M. Leunig, and R. K. Jain. 1993. Fluorescence photobleaching with spatial Fourier analysis: measurement of diffusion in light-scattering media. *Biophys. J.* 65:2428–2436.

Bor Fuh, C., S. Levin, and J. C. Giddings. 1993. Rapid diffusion coefficient measurements using analytical SPLITT fractionation: application to proteins. *Anal. Biochem.* 208:80–87.

Boyer, P. M., and J. T. Hsu. 1992. Experimental studies of restricted protein diffusion in an agarose matrix. *AIChE J.* 38:259–272.

Brigham, E. O. 1974. The Fast Fourier Transform. Prentice-Hall, Englewood Cliffs, NJ. 140–147.

Crone, H. D. 1974. Ion-exclusion effects on the chromatography of acetylcholinesterase and other proteins on agarose columns at low ionic strengths. *J. Chromatogr.* 92:127–135.

Djabourov, M., A. H. Clark, D. W. Rowlands, and S. B. Ross-Murphy. 1989. Small-angle x-ray scattering characterization of agarose sols and gels. *Macromol. Rev.* 22:180–188.

Dubin, P. L., and J. M. Principi. 1989. Optimization of size-exclusion separation of proteins on a Superose column. *J. Chromatogr.* 479: 159–164.

Fanti, L. A., and E. D. Glandt. 1990. Partitioning of spherical particles into fibrous matrices. *J. Colloid Interface Sci.* 135:385–395.

Gaigalas, A. K., J. B. Hubbard, M. McCurley, and S. Woo. 1992. Diffusion of bovine serum albumin in aqueous solutions. *J. Phys. Chem.* 96:2355–2359.

Gibbs, S. J., A. S. Chu, E. N. Lightfoot, and T. W. Root. 1991. Ovalbumin diffusion at low ionic strength. *J. Phys. Chem.* 95:467–471.

Giddings, J. C., F. J. F. Yang, and M. N. Myers. 1976. Flow field-flow fractionation: a versatile new separation method. *Science.* 193: 1244–1245.

Gordon, W. G., and W. F. Semmett. 1953. Isolation of crystalline a-lactalbumin from milk. *J. Am. Chem. Soc.* 75:328–330.

Haugland, R. 1992–1994. Molecular Probes: Handbook of Fluorescent Probes and Research Chemicals, 5th ed. Molecular Probes, Eugene, OR.

Jackson, G. W., and D. F. James. 1986. The permeability of fibrous porous media. *Can. J. Chem. Eng.* 64:364–374.

Jain, R. K., R. J. Stock, S. R. Chary, and M. Rueter. 1990. Convection and diffusion measurements using fluorescence recovery after photobleaching and video image analysis: in vitro calibration and assessment. *Microvasc. Res.* 39:77–93.

Johnson, K. A., G. B. Westermann-Clark, and D. O. Shah. 1989. Diffusion of charged micelles through charged microporous membranes. *Langmuir.* 5:932–938.

Larson, R. J., and M. L. Marx. 1986. An Introduction to Mathematical Statistics and Its Applications, 2nd ed. Prentice-Hall, Englewood Cliffs, NJ.

Laurent, T. C. 1967. Determination of the structure of agarose gels by gel chromatography. *Biochim. Biophys. Acta.* 136:199–205.

Lin, N. P., and W. M. Deen. 1992. Charge effects on the diffusion of polystyrene sulfonate through porous membranes. *J. Colloid Interface Sci.* 153:483–492.

Moussaoui, M., M. Benlyas, and P. Wahl. 1992. Diffusion of proteins in Sepharose Cl-B gels. *J. Chromatogr.* 591:115–120.

Obrink, B. 1968. Characterization of fiber parameters in agarose gels by light scattering. *J. Chromatogr.* 37:329–330.

Ogston, A. G. 1958. The spaces in a uniform random suspension of fibers. *Trans. Faraday Soc.* 54:1754–1757.

Ogston, A. G., B. N. Preston, and J. D. Wells. 1973. On the transport of compact particles through solutions of chain polymers. *Proc. R. Soc. Lond. A.* 333:297–316.

Overbeek, J. T. G. 1950. Quantitative interpretation of the electrophoretic velocity of colloids. *In* Advances in Colloid Science, Vol. III. H. Mark and J. W. Verwey, editors. Interscience Publishers, New York. 97–133.

Phillies, G. D. J., C. Malone, K. Ullmann, G. S. Ullmann, J. Rollings, and L. Yu. 1987. Probe diffusion in solutions of long-chain polyelectrolytes. *Macromol. Rev.* 20:2280–2289.

Phillies, G. D. J., T. Pirnat, M. Kiss, N. Teasdale, D. Maclung, H. Inglefield, C. Malone, A. Rau, L. Yu, and J. Rollings, 1989. Probe diffusion in solutions of low molecular weight polyelectrolytes. *Macromol. Rev.* 22: 4068–4075.

Phillips, R. J., W. M. Deen, and J. F. Brady. 1989. Hindered transport in fibrous membranes and gels: effect of solute size and fiber configuration. *AIChE J.* 35:1761–1769.

Raj, T., and W. H. Flygare. 1974. Diffusion studies of bovine serum albumin by quasi-elastic light scattering. *Biochemistry.* 13:3336–3340.

Righetti, P. G., and T. Caravaggio. 1976. Isoelectric points and molecular weights of proteins: a table. *J. Chromatogr.* 127:1–28.

Sellen, D. B. 1973. Light scattering Rayleigh linewidth measurements on some globular protein solutions. *Polymers.* 14:359–364.

Sellen, D. B. 1985. Quasi-elastic light scattering studies of the diffusion of compact macromolecules through gels. *In* Physical Optics of Dynamic Phenomena and Processes in Macromolecular Systems. B. Sedlacek, editor. DeGruyter, Berlin, Germany. 177–190.

Shukla, T. P. 1973. Chemistry and biological function of a-lactalbumin. *CRC Crit. Rev. Food Technol.* 3:241–312.

Spencer, M. 1982. Reverse salt gradient chromatography of tRNA on unsubstituted agarose. III. Physical and chemical properties of different batches of Sepharose 4B. *J. Chromatogr.* 238:317–325.

Tanford, C., S. A. Swanson, W. S. Shore. 1955. Hydrogen ion equilibria of bovine serum albumin. *J. Am. Chem Soc.* 77:6414–6421.

Tsay, T. T., and K. A. Jacobson. 1991. Spatial Fourier analysis of video photobleaching measurements: principles and optimization. *Biophys. J.* 60:360–368.

Waki, S., J. D. Harvey, and A. R. Bellamy. 1982. Study of agarose gels by electron microscopy of freeze-fractured surfaces. *Biopolymers.* 21:1909–1926.

Walters, R. R., J. F. Graham, R. M. Moore, and D. J. Anderson. 1984. Protein diffusion coefficient measurements by laminar flow analysis: method and applications. *Anal. Biochem.* 140:190–195.

Wattenbarger, M. R., V. A. Bloomfield, Z. Bu, and P. S. Russo. 1992. Tracer diffusion of proteins in DNA solutions. *Macromolecules.* 25:5263–5265.

Weast, R. C., and M. J. Astle, editors. 1980. CRC Handbook of Chemistry and Physics, 61st ed. CRC Press Inc., Boca Raton, FL. F-51.

Whytock, S., and J. Finch. 1991. The substructure of agarose gels as prepared for electrophoresis. *Biopolymers.* 31:1025–1028.